Int J Mater Form (2010) 3:103–115
DOI 10.1007/s12289-009-0660-0

ORIGINAL RESEARCH

An analysis of wrinkling limit diagrams of aluminum alloy 5005 annealed at different temperatures

R. Ravindran · K. Manonmani · R. Narayanasmay

Received: 21 May 2009 / Accepted: 16 September 2009 / Published online: 7 October 2009

Abstract This paper deals with the wrinkling limit diagrams for Aluminum alloy 5005 sheets having thickness of 2.00 mm annealed at four different temperatures namely 200°C, 300°C, 400°C and 500°C. The study pertains to deep drawing into cylindrical cups through conical die using a flat bottom punch. It is proved by these researchers and others that the onset of wrinkling takes place when the ratio of strain increments ($d\varepsilon_r$ / $d\varepsilon_\theta$) or the ratio of strain (ε_r / ε_θ) reaches a critical value during the drawing process. These values which could be determined experimentally over which the wrinkling takes place, is shown in the form of wrinkling limit diagrams for the above grade at different annealing temperature. An attempt is also made to develop the wrinkling theory that predicts the wrinkling based on results obtained in the form of wrinkling limit diagrams established for the above grade at different annealed temperature. Further it has been observed from the stress ratio that there is a clear curve, that separates the region from safe and the wrinkling region. Further it was observed that the annealed sheets having high n-value, high R-value and high UTS /σ_y ratio improve the resistance against wrinkling.

Keywords Wrinkling limit diagrams · Strain increments ratio · Strain ratio · Stress ratio · Conical die

R. Ravindran (✉)
Department of Mechanical Engineering,
Dr. Mahalingam College of Engineering & Technology,
Pollachi 642003, Tamilnadu, India
e-mail: mceravindran@yahoo.co.in

K. Manonmani
Department of Mechanical Engineering,
Government college of Technology,
Coimbatore 641013, Tamilnadu, India

R. Narayanasmay
Department of Production Engineering,
National Institute of Technology,
Tiruchirappalli 620 015, Tamil Nadu, India

Nomenclature

n_{av}	– average strain hardening index value.
n_{av}	$= 0.25(n_0 + 2n_{45} + n_{90})$
k_{av}	– average strength coefficient.
k_{av}	$= 0.25(k_0 + 2k_{45} + k_{90})$
R	– average normal anisotropy
R	$= 0.25(R_0 + 2R_{45} + R_{90})$
x_{av}	$= 0.25(x_0 + 2x_{45} + x_{90})$
σ_Y (average)	$= 0.25(\sigma_{Y0} + 2\sigma_{Y45} + \sigma_{Y90})$
σ_U (average)	$= 0.25(\sigma_{U0} + 2\sigma_{U45} + \sigma_{U90})$
σ_r	- Radial stress
σ_θ	- Hoop stress
$\overline{\sigma}$	- Effective stress
ε_r	- Radial strain
ε_θ	- Hoop strain
$\overline{\varepsilon}$	- Effective strain
$d\sigma_r$	- Radial stress increment
$d\sigma_\theta$	- Hoop stress increment
$d\varepsilon_r$	- Radial strain increment
$d\varepsilon_\theta$	- Hoop strain increment
$d\overline{\varepsilon}$	- Effective strain increment
$d\gamma_{max}$	- Maximum shear strain increment
γ_{max}	- Maximum shear strain
τ_{max}	- Maximum shear stress
α	- Ratio of in plane stress increments
β	- Ratio of in plane strain increments
a	- Yielding behaviour constant

Introduction

Influence of annealing of commercially pure (CP) Aluminum was evaluated by aspects namely microstructure, mechanical properties, electrical conductivity, and general corrosion. It is shown that by selecting optimal annealing condition result in ultra fine grains in CP Aluminum with good combination of high strength and ductility as explained elsewhere [1]. Using an Al-Mg-Cu alloy developed for auto body panels, strip sheets are experimentally produced by various cold-rolling and annealing procedures. Tensile and metallographic properties of the sheets and their relations are examined to attain high formability. The elongation is closely related to the grain size, and increases with the final annealing temperature as described by H. Takuda [2]. In sheet metal forming, production engineers and researchers have paid much attention to the behaviour of wrinkling in sheet metal forming operations over the last decade. It is difficult to define criteria for describing the stability in metal forming. In general, wrinkling may be affected by various factors including material properties, punch and die geometry, blank geometry, holding conditions, interface friction and lubrication state. Numerous studies have been carried out on the relationship between wrinkling and material characteristics. Karima and Sowerby [3] have attempted a bifurcation approach to the study of wrinkling during deep drawing. They treated flange wrinkling during deep drawing without a blank holder as a problem of elastic-plastic buckling of an annular plate. Their results indicate that a high rate of hardening has a favourable effect on the prevention of buckling when deep drawing through Conical and tapered dies. However, Narayanasamy and Sowerby [4] has showed that the stainless steel 304 sheets which have a low value of normal anisotropy and a high value of normalized hardening rate, have better resistance to the formation of wrinkles. Di and Thomson [5] have used the neural network principle for the prediction of strain at the onset of wrinkling, based on the Yoshida material parameters. The effect of geometrical variables that affect the onset of wrinkling during deep drawing has been investigated by Wang et al. [6], using a neural network approach.

Kim and Son [7] studied wrinkling behaviour of sheet metals using a numerical analysis for evaluating a wrinkling limit diagram (WLD) for an anisotropic sheet subjected to biaxial plane stress. The scheme of plastic bifurcation theory for thin shells based on the Donnell-Mushtari-Vlasov shell theory is used. The effects of various material parameters namely yield stress, strain hardening coefficient, and normal anisotropy and geometrical parameters on the wrinkling limit diagram where investigated numerically and compared with the results of the experiments of Kawai and Havrnek. The formation of wrinkles can be predicted by analytical treatments using Hill's [8] bifurcation criterion, specialized by Hutchinson [9] to the case of thin and shallow plates and shells.

In the present work, an attempt is made to predict the onset of wrinkling using wrinkling limit diagram for Aluminum alloy 5005 at different annealed temperatures.

Experimental work

Cold rolled Aluminum alloy 5005 sheet metal having thickness 2.00 mm were subjected to four different annealing treatments namely (1) heating temperature 200°C, soaking (maintaining constant temperature in the furnace) time 1 hr and furnace cooling (HT1), (2) heating temperature 300°C, soaking time 1 hr and furnace cooling (HT2), (3) heating temperature 400°C, soaking time 1 hr and furnace cooling (HT3) and (4) heating temperature 500°C, soaking time 1 hr and furnace cooling (HT4). An ordinary muffle furnace was used for heating the Aluminum alloy sheets. The metallurgical microstructure of Aluminum alloy 5005 annealed at four different temperatures are provided in Fig. 1. Table 1 shows the chemical composition of the above said sheet metal and their mechanical properties at different annealing temperatures were tabulated in Tables 2, 3, 4, 5. Since the sheet metals are anisotropy in nature, the normal anisotropy parameter (R) was evaluated as shown in Ref. [7, 8]. This is defined as

$$R = 0.25(R_0 + 2R_{45} + R_{90}) \tag{1}$$

Where 0, 45 and 90 represents rolling direction, 45° to rolling direction and transverse direction respectively. R is the plastic strain ratio. Tables 2, 3, 4, 5, present some typical results of the R values obtained for the annealed Aluminum alloy 5005 grade with four different heat treated conditions. The value of strain increment ratio for different R values were tabulated in Table 6. The drawing experiments were also conducted as per schedule described elsewhere [4], using Conical die for the four different heat-treated Aluminum alloy 5005 grade (Fig. 2). The blanks having different diameters were drawn through the die with no lubricant. A grid consisting of circles of 3.5 mm in diameter was printed on the blanks for the determination of the strain distribution. The grid circles were printed on blanks by using electro chemical etching process. The grid measurements reveal the onset of wrinkling in the stage of bending or tube sinking. The blanks were partially drawn through the die to about ten or more different depths until the wrinkling developed and the grid circles measured on each of the partially drawn sheets in a region close to the rim of the blank where wrinkling generally developed. The strains, namely, hoop (ε_θ) and radial (ε_r) were calculated from the grid measurement data. Figures 4a–d show the sample distribution of the radial and hoop strains for different Aluminum alloy blanks of grade Aluminum alloy 5005 which is subjected to four different types of heat treatments as said above. From these Figures it is noted that the slope of the ε_r–ε_θ strain curve changes suddenly when a wrinkle develops on the blank. The reason for this is that there is an increase in circumferential strain (ε_θ) when the wrinkle is about to develop on the blank (Fig. 4).

Theoretical analysis

Theory of plasticity

The wall section of a truncated Conical cup (a partially drawn cup) is approximated to a flat strip of width 'a_1' and height 'b_1' as shown in the Fig. 3a, corresponding respectively to the mean circumference and the generator of the cone. The strip is subjected to plane stress, specified by σ_r and σ_θ. as shown in Fig. 3b

Assuming the material to be rigid-plastic and obeying the Hill new yield criterion [8] together with the Levy-Mises flow rule, the increments of strain can be expressed as follows:

$$\begin{aligned} d\varepsilon_1 &= d\lambda\left[(\sigma_1+\sigma_2)^{a-1}+(1+2R)(\sigma_1-\sigma_2)^{a-1}\right] \\ d\varepsilon_2 &= d\lambda\left[(\sigma_1+\sigma_2)^{a-1}+(1+2R)(\sigma_1-\sigma_2)^{a-1}\right] \\ d\varepsilon_3 &= -d\lambda\left[2(\sigma_1+\sigma_2)^{a-1}\right] \end{aligned} \tag{2}$$

Where 'a' is yielding behaviour constant.

The ratio of the in-plane strain increments can be expressed as

$$\frac{d\varepsilon_2}{d\varepsilon_1} = \frac{(\sigma_1+\sigma_2)^{a-1}-(1+2R)(\sigma_1-\sigma_2)^{a-1}}{(\sigma_1+\sigma_2)^{a-1}+(1+2R)(\sigma_1-\sigma_2)^{a-1}} \tag{3}$$

Expression (3) can be rewritten as

$$\beta = \frac{(1+\alpha)^{a-1}-(1+2R)(1-\alpha)^{a-1}}{\left((1+\alpha)^{a-1}+(1+2R)(1-\alpha)^{a-1}\right.} \tag{4}$$

where

$$\alpha = \frac{\sigma_2}{\sigma_1} = \frac{\sigma_\theta}{\sigma_r} \quad \text{and} \quad \beta = \frac{d\varepsilon_2}{d\varepsilon_1} = \frac{d\varepsilon_\theta}{d\varepsilon_r} \tag{5}$$

The constant 'a' provided in the Eqs. (2)–(4) represents the yielding behaviour of metals.

The quantities α and β are the ratios of the in-plane stress and the in-plane plastic strain increments, respectively. Hence, if the ratio of the stress is known the ratio of the strain increments can be determined and vice versa. For wrinkling to occur it is necessary that σ_θ should be compressive (i.e. α should be negative).

As per Hill's old yield criterion [8], putting a=2, expression (4) becomes

$$\beta = \frac{(1+\alpha)-(1+2R)(1-\alpha)}{((1+\alpha)+(1+2R)(1-\alpha)} \tag{6}$$

In expression (6) α takes the value of zero to infinity. Substituting the limiting values

$$\begin{aligned} \beta &= \frac{-R}{1+R} \quad (when\, \alpha = 0) \\ &and \\ \beta &= \frac{-(1+R)}{R} \quad (when\, \alpha = \infty) \end{aligned} \tag{7}$$

When R takes the value of unity:

$$-2 < \beta < -1/2 \tag{8}$$

This relationship is true irrespective of whether the material work-hardens or not. The above relationship [refer Eq. (7)] is independent of the yielding behaviour constant 'a'. This can be checked without substituting the value of 2.0 for the above constant 'a', in the Eq. (4), provided in the above. As shown in Fig. 3b, this situation can be represented in principal stress space and principal strain space.

The Eq. (6) can be rearranged as follows:

$$\alpha = \frac{R(1+\beta)+\beta}{R(1+\beta)+1} \tag{9}$$

Using the Eq. (9), for the known values of β and R, the value of α can be determined.

As described elsewhere [10], the effective strain increment can be written as follows:

$$d\bar{\varepsilon} = \sqrt{2/3}\left[\frac{(2+R)(1+R)}{(1+2R)}\left\{d\varepsilon_r^2 + d\varepsilon_\theta^2 + \left(\frac{2R}{1+R}\right)d\varepsilon_r d\varepsilon_\theta\right\}\right]^{0.5} \tag{10}$$

The Eq. (10) can also be written as follows:

$$\frac{d\bar{\varepsilon}}{d\varepsilon_r} = \sqrt{2/3}\left[\frac{(2+R)(1+R)}{(1+2R)}\left\{1 + \left(\frac{d\varepsilon_\theta}{d\varepsilon_r}\right)^2 + \left(\frac{2R}{1+R}\right)\frac{d\varepsilon_\theta}{d\varepsilon_r}\right\}\right]^{0.5} \tag{11a}$$

Similarly,

$$\frac{d\bar{\varepsilon}}{d\varepsilon_\theta} = \sqrt{2/3}\left[\frac{(2+R)(1+R)}{(1+2R)}\left\{1 + \left(\frac{d\varepsilon_r}{d\varepsilon_\theta}\right)^2 + \left(\frac{2R}{1+R}\right)\frac{d\varepsilon_r}{d\varepsilon_\theta}\right\}\right]^{0.5} \tag{11b}$$

For the known values of $d\varepsilon_r$ and $d\varepsilon_\theta$, the effective strain increment $d\bar{\varepsilon}$, the ratio $\left(\frac{d\bar{\varepsilon}}{d\varepsilon_r}\right)$ and the ratio $\left(\frac{d\bar{\varepsilon}}{d\varepsilon_\theta}\right)$ can be determined.

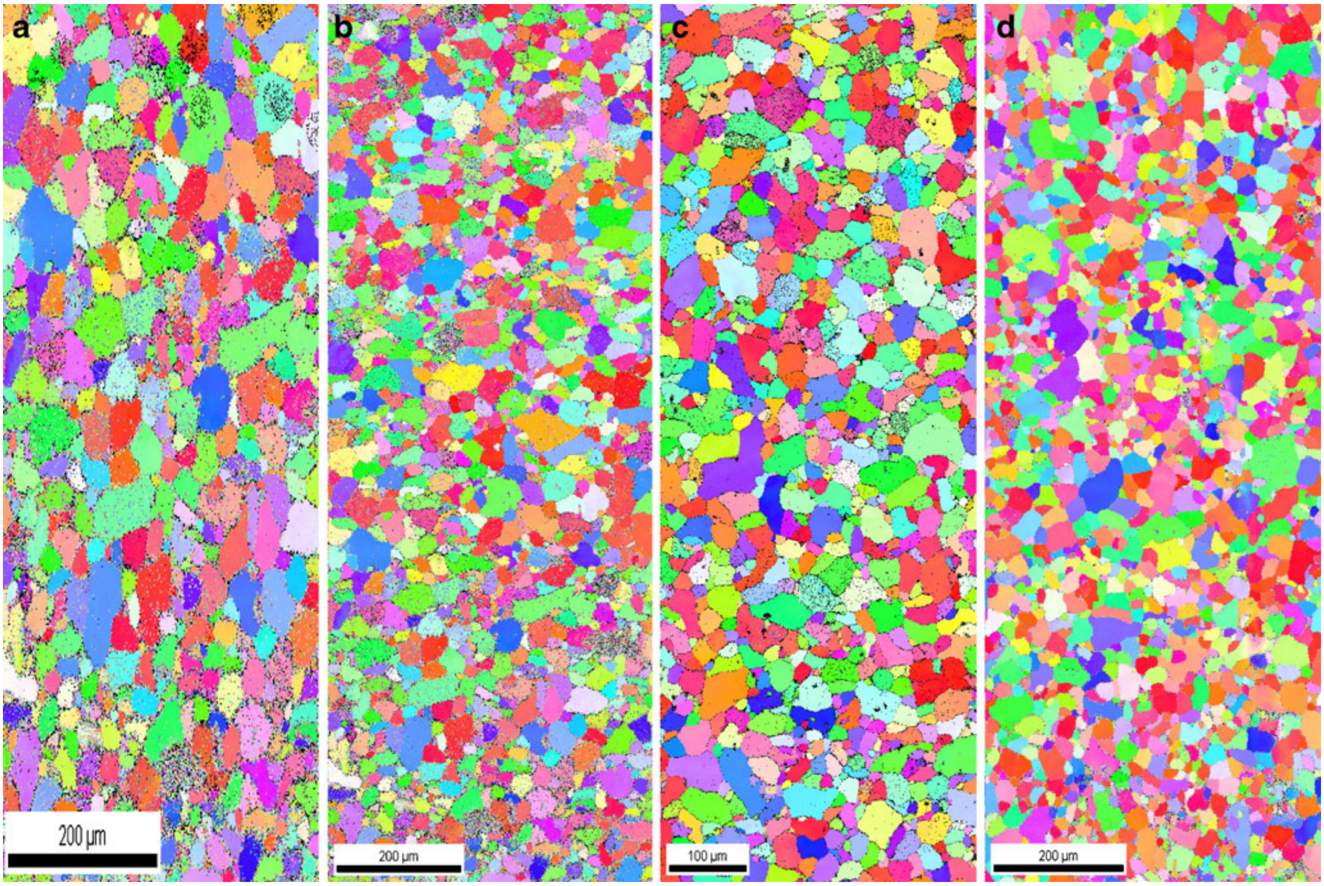

Fig. 1 **a** Microstructure of aluminum alloy 5005 annealed at 200°C. **b** Microstructure of aluminum alloy 5005 annealed at 300°C. **c** Microstructure of aluminum alloy 5005 annealed at 400°C. **d** Microstructure of aluminum alloy 5005 annealed at 500°C

As described elsewhere [10], the yield function can be described as follows:

$$\sigma_r^2 + \sigma_\theta^2 - \left(\frac{2R}{1+R}\right)\sigma_r\sigma_\theta = \overline{\sigma}^2 \tag{12}$$

The Eq. (12) can be described as follows:

$$\left(\frac{\sigma_r}{\overline{\sigma}}\right)^2 = \left(1 + \alpha_1^2 - \frac{2R\alpha_1}{(1+R)}\right)^{-1} \tag{13a}$$

and

$$\left(\frac{\sigma_\theta}{\overline{\sigma}}\right)^2 = \left(1 + \alpha_2^2 - \frac{2R\alpha_2}{(1+R)}\right)^{-1} \tag{13b}$$

Where,

σ_r is the radial stress
σ_θ is the hoop stress
$\overline{\sigma}$ is the effective stress
R is the normal anisotropy
α_1 $= \sigma_\theta/\sigma_r$ and
α_2 $= \sigma_r/\sigma_\theta$

From Eqs. (13a) and (13b) for known values of α_1, α_2 and R, the stress ratios $(\sigma_r/\overline{\sigma})$ and $(\sigma_\theta/\overline{\sigma})$ can be determined.

For sheet metals used in industries, the value of R (the normal anisotropy) varies from 0.25 to 3.00. Therefore, the limiting strain increments ratio (β) can be determined using Eq. (7) and the same is reported in Table 3. Table 3 shows that the strain increments ratio value depends upon R value only. However, it is already proved by Narayanasamy and Sowerby [4] that the strain increments ratio value also depends upon the strain hardening exponent value apart from R-value for the case of austenitic stainless steels (grades 301, 302 and 304) due to the formation of plastically strain induced martensite.

Table 1 Chemical composition of aluminum alloy 5005 (in wt %)

Material	Mg	Mn	Si	Fe	Cr	Cu	Zn	Al
Al 5005 alloy	1.1	0.2	0.3	0.7	0.1	0.2	0.25	Rest

Table 2 Tensile properties of aluminum alloy 5005 annealed at 200°C

Orientation relative to rolling direction	Strain hardening exponent n	Strength coefficient KMPa	R	Yield stress (σ_y) MPa	Ultimate tensile stress in MPa	UTS/σ_y	% elongation
0°	0.178	420	0.940	251 average	275.54 average	1.09	12.71
45°	0.095	390					
90°	0.17	440					
Average[a]	0.155	410					

[a] Average $= (X_0 + 2X_{45} + X_{90})/4$, where x is n-value or K-value

According to Mohr's circle drawn between $d\varepsilon_r$ (the radial strain increments) and $d\varepsilon_\theta$ (the hoop strain increment), the following expression can be written.

$$d\gamma_{\max} = \frac{1}{2}(d\varepsilon_r + d\varepsilon_\theta) \tag{14}$$

Where $d\gamma_{\max}$ represents the maximum shear strain increment value, which is nothing but the radius of Mohr's circle.

The Eq. (14) can be written as follows:

$$\begin{aligned} \frac{d\gamma_{\max}}{d\varepsilon_\theta} &= \frac{1}{2}\left[\frac{d\varepsilon_r}{d\varepsilon_\theta} + 1\right] \\ \frac{d\gamma_{\max}}{d\varepsilon_r} &= \frac{1}{2}\left[\frac{d\varepsilon_\theta}{d\varepsilon_r} + 1\right] \end{aligned} \tag{15}$$

Since the value of $(d\varepsilon_r / d\varepsilon_\theta)$ is known, the values of $\frac{d\gamma_{\max}}{d\varepsilon_\theta}$ and $\frac{d\gamma_{\max}}{d\varepsilon_r}$ can be determined using Eq. (15). If we assume that the strain proportional, then

$$\frac{d\varepsilon_\theta}{d\varepsilon_r} = \frac{\varepsilon_\theta}{\varepsilon_r} \tag{16}$$

Therefore, the Eq. (15) can be modified as follows

$$\begin{aligned} \frac{\gamma_{\max}}{\varepsilon_\theta} &= \frac{1}{2}\left[\frac{\varepsilon_r}{\varepsilon_\theta} + 1\right] \\ \frac{\gamma_{\max}}{\varepsilon_r} &= \frac{1}{2}\left[\frac{\varepsilon_\theta}{\varepsilon_r} + 1\right] \end{aligned} \tag{17}$$

Since the deformation is under plane stress, only stresses namely σ_r and σ_θ are present. Therefore, the following expressions can be written with similar to Eqs. (15) and (17).

$$\begin{aligned} \frac{\tau_{\max}}{\sigma_\theta} &= \frac{1}{2}\left[\frac{\sigma_r}{\sigma_\theta} + 1\right] \\ \frac{\tau_{\max}}{\sigma_r} &= \frac{1}{2}\left[\frac{\sigma_\theta}{\sigma_r} + 1\right] \end{aligned} \tag{18}$$

Here, $\tau_{\max}$ is the maximum shear stress developed, which is nothing but the radius of the Mohr's circle.

The Eq. (10) can be written as follows for the determination of the effective strain providing the strain is proportional.

$$\overline{\varepsilon} = \sqrt{2/3}\left[\frac{(2+R)(1+R)}{(1+2R)}\left\{\varepsilon_r^2 + \varepsilon_\theta^2 +\right)\left(\frac{2R}{1+R}\right)\varepsilon_r\varepsilon_\theta\right\}\right]^{0.5} \tag{19}$$

The Eq. (19) can be rearranged as follows:

$$\frac{\overline{\varepsilon}}{\varepsilon_r} = \sqrt{2/3}\left[\frac{(2+R)(1+R)}{(1+2R)}\left\{1 + \left(\frac{\varepsilon_\theta}{\varepsilon_r}\right)^2 + \left(\frac{2R}{1+R}\right)\frac{\varepsilon_\theta}{\varepsilon_r}\right\}\right]^{0.5} \tag{20a}$$

$$\frac{\overline{\varepsilon}}{\varepsilon_\theta} = \sqrt{2/3}\left[\frac{(2+R)(1+R)}{(1+2R)}\left\{1 + \left(\frac{\varepsilon_r}{\varepsilon_\theta}\right)^2 + \left(\frac{2R}{1+R}\right)\frac{\varepsilon_r}{\varepsilon_\theta}\right\}\right]^{0.5} \tag{20b}$$

For known values of ε_r and ε_θ, the effective strain $(\overline{\varepsilon})$ and strain ratios namely $\left(\frac{\overline{\varepsilon}}{\varepsilon_r}\right)$ and $\left(\frac{\overline{\varepsilon}}{\varepsilon_\theta}\right)$ can be determined.

Results and discussion

Chemical composition and microstructure

The chemical composition for Aluminum alloy 5005 alloy tested is provided in Table 1, and the metallurgical

Table 3 Tensile properties of aluminum alloy 5005 annealed at 300°C

Orientation relative to rolling direction	Strain hardening exponent n	Strength coefficient KMPa	R	Yield stress (σ_y) MPa	Ultimate tensile stress in MPa	UTS/σ_y	% elongation
0°	0.212	410	0.98	245 average	268.28 average	1.095	13.62
45°	0.115	440					
90°	0.22	450					
Average[a]	0.166	435					

[b] Average $= (X_0 + 2X_{45} + X_{90})/4$, where x is n-value or K-value

Table 4 Tensile properties of aluminum alloy 5005 annealed at 400°C

Orientation relative to rolling direction	Strain hardening exponent n	Strength coefficient KMPa	R	Yield stress (σ_y) MPa	Ultimate tensile stress in MPa	UTS/σ_y	% elongation
0°	0.176	410	1.1	222 average	260.52 average	1.17	14.82
45°	0.188	490					
90°	0.172	450					
Average[a]	0.181	460					

[a] Average $= (X_0 + 2X_{45} + X_{90})/4$, where x is n-value or K-value

microstructure of Aluminum alloy 5005 annealed at four different temperatures details are provided in Fig. 1. The microstructure of the sheet annealed at 200°C shows partial recovery and no recrystallization. The microstructure of sheets annealed at 300°C and 400°C shows fully recovered and partial recrystallized grain structure whereas, sheets annealed at 500°C shows completely recrystallized grains which is clearly seen in Fig. 1. A fundamental understanding 5005 is a medium to high strength non-heat-treatable alloy. The alloy has good formability than alloy 5083. The magnesium in the Aluminum alloy 5005 is 4.0 %, the presence of magnesium in larger quantity retards formability but enhances castability and strength. The percentage of iron in the material is 0.50%, its presence in the alloy increase the recrystallisation temperature. The presence of silicon is about 0.4% and its improves the fluidity of the alloy. The manganese and chromium jointly counteract the corrosion effect of Iron. Manganese and chromium have a strengthening effect with reduction of ductility. Copper content is about 0.10% and its presence, reduces pitting corrosion. The zinc that is present in 0.25% does not have effect on corrosion but enhances castability and strength. Iron may form $FeAl_3$ in the absence of chromium or manganese. Titanium remains mostly in solution. Titanium increases the recrystallisation temperature and aids in grain refinement.

Tensile properties

Tensile properties of sheets annealed at four different temperatures are shown in Tables 2, 3, 4 and 5. The average strain hardening exponent ($\overline{n}$) value indicates stretchability and formability [11, 12]. As the $\overline{n}$-value increases, the stretchability also increases. The sheets annealed at 200°C, possess comparatively less average strength coefficient value (K) due to presence of cold worked microstructure. Whereas, the grains in microstructure of the sheets annealed at 500°C is recrystallized in nature and they possess high average strength coefficient (K). The sheets annealed at 500°C temperature possess a lower value of UTS, compared to other lower annealing temperatures.

Wrinkling limit diagram

The ratio of strain increments ($d\varepsilon_r/d\varepsilon_\theta$) and the ratio of strains (ε_r / ε_θ) at the onset of wrinkling can be obtained from the strain values namely ε_r and ε_θ measured for the drawing operation. The same is shown in the form of diagrams in Figs. 4a–d. Using the expressions provided by the theory of plasticity, the wrinkling limit diagrams in terms of strain increments ratio, strain ratio and stress ratio can be plotted as shown in this section.

Figure 5 has been plotted between the strain increments ratio ($d\varepsilon_r/d\varepsilon_\theta$) and the effective strain increment for the case of drawing of Aluminum alloy 5005 sheets annealed at 200°C, 300°C, 400°C and 500°C through the conical die. It is observed that the strain increments ratio obtained at the onset of wrinkling is found to be higher value for the Aluminum alloy 5005 sheet annealed at 500°C comparing to other three annealed temperature namely 200°C, 300°C and 400°C. Further, it is observed that the area of safe region is found to be greater for annealed temperature of 500°C and lower for 200°C. The behaviour of Aluminum

Table 5 Tensile properties of aluminum alloy 5005 annealed at 500°C

Orientation relative to rolling direction	Strain hardening exponent n	Strength coefficient KMPa	R	Yield stress (σ_y) MPa	Ultimate tensile stress in MPa	UTS/σ_y	% elongation
0°	0.259	480	1.128	210 average	253.32 average	1.206	15.2
45°	0.261	550					
90°	0.142	460					
Average[a]	0.231	510					

[a] Average $= (X_0 + 2X_{45} + X_{90})/4$, where x is n-value or K-value

Table 6 Values of strain increments ratio (β) for various R values

R-Value	β-value when	
	α=0.0	α=∞
0.00	0.000	Infinity
0.25	0.200	5.000
0.50	0.333	3.000
0.75	0.4285	2.334
1.00	0.500	2.000
1.50	0.600	1.667
2.00	0.666	1.500
2.50	0.7142	1.400
3.00	0.750	1.333

This table is derived using Eq. (7) explained in the text. Normal anisotropy (R) takes values from 0.25 to 3.0 for industrial sheet metals

alloy 5005 annealed at 300°C and 400°C is in between that sheets annealed at 200°C and 500°C.

Figure 6 has been plotted between the stress ratio, $(\sigma_r/\overline{\sigma})$, and the stress ratio, $(\sigma_\theta/\overline{\sigma})$, for the onset of wrinkling when drawing through the conical die for the Aluminum alloy 5005 sheet annealed at four temperatures namely 200°C, 300°C, 400°C and 500°C. It is observed that there is a clear curve, which separates the region from safe and the wrinkling region. The ratio of (σ_θ/σ_r) is found to be 1.29.

Figure 7 has been plotted between the strain ratio $(\overline{\varepsilon}/\varepsilon_r)$ and the strain ratio $(\overline{\varepsilon}/\varepsilon_\theta)$, for Aluminum alloy 5005 sheet annealed at four different temperatures drawn through Conical die. As said earlier, there is a clear demarcation curve between the safe region and the wrinkling region. This demonstrates that the Aluminum alloy 5005 sheet annealed at 500°C accommodates more hoop strain and radial strains before the onset of wrinkling comparing to the other two temperatures. The safe region is found to be more for higher annealing temperature (500°C).

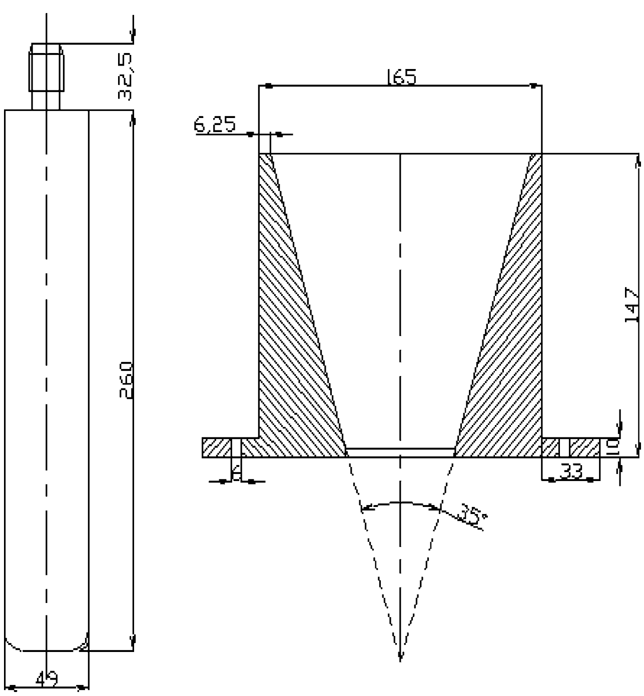

Fig. 2 Conical die and flat bottomed punch

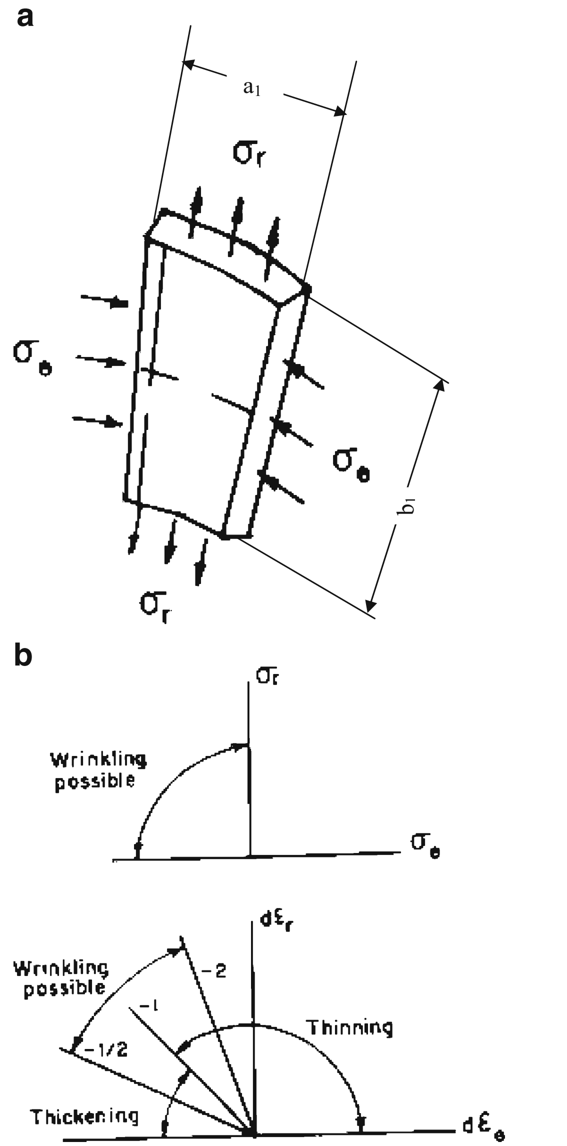

Fig. 3 **a** Stress State in the Cup Wall. (a_1 and b_1 represents the dimensions namely width and height). **b** Wrinkling tendencies shown in stress and strain space

Figure 8 has been plotted between the strain increment ratio $(d\overline{\varepsilon}/d\varepsilon_r)$ and the strain increment ratio $(d\overline{\varepsilon}/d\varepsilon_\theta)$ obtained using Eq. (11a), for four different annealed temperature for Aluminum alloy 5005 when drawn through Conical die. For Aluminum alloy 5005 sheet annealed at 500°C, the safe region is found to be the highest and whereas for annealed at 200°C the same region is found to be the lowest.

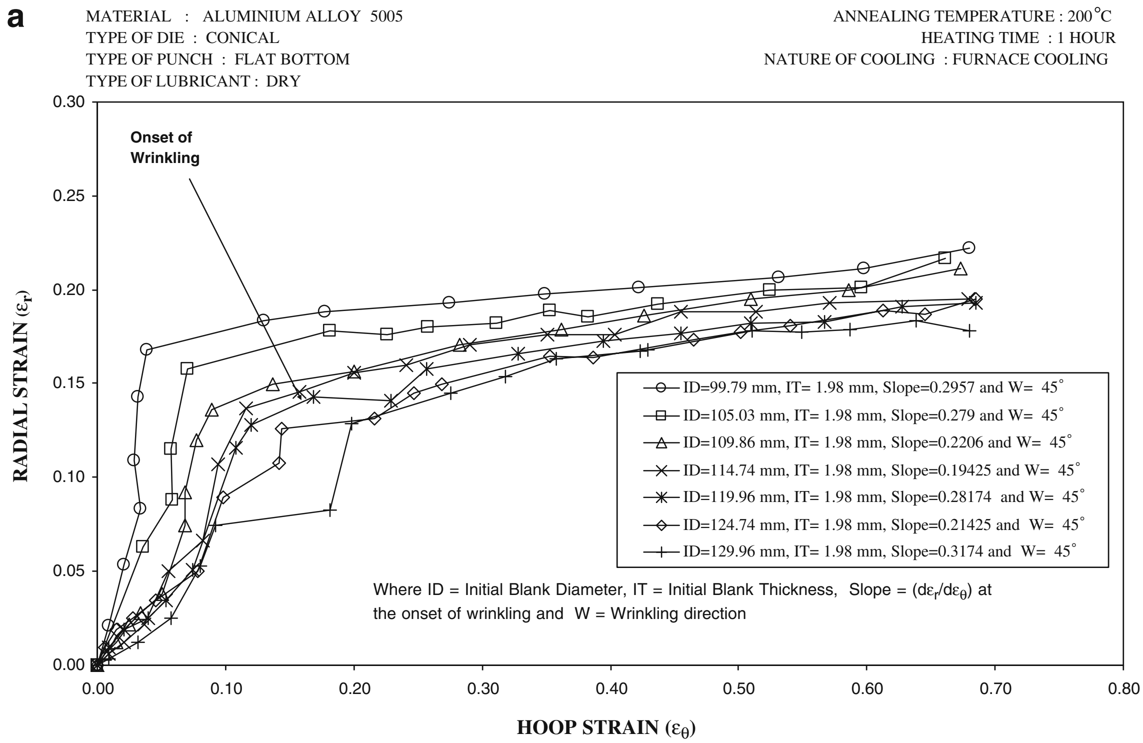

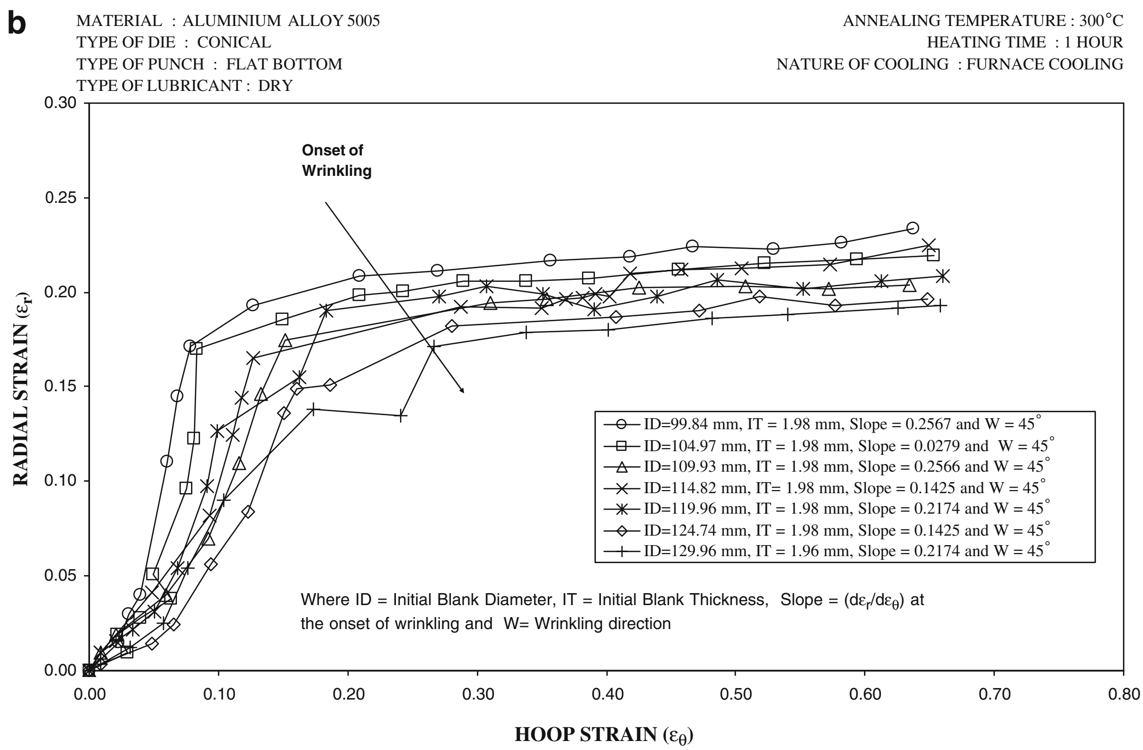

Fig. 4 a–d Variation of the radial strain with respect to the hoop strain

Figure 9 has been plotted between the strain increments ratio $(d\gamma_{max}/d\varepsilon_r)$ and the strain increments ratio $(d\gamma_{max}/d\varepsilon_\theta)$ for four different annealed temperature for Aluminum alloy 5005 when drawn through Conical die. It is observed that the strain increments ratio values obtained at the onset of wrinkling is found to fall in a single curve for four different annealed temperature for Aluminum alloy 5005. The wrinkling takes place over the strain increment $(d\gamma_{max}/d\varepsilon_\theta)$ range from 0.72 to 1.6 for the Conical die and there is a clear demarcation curve between the safe region

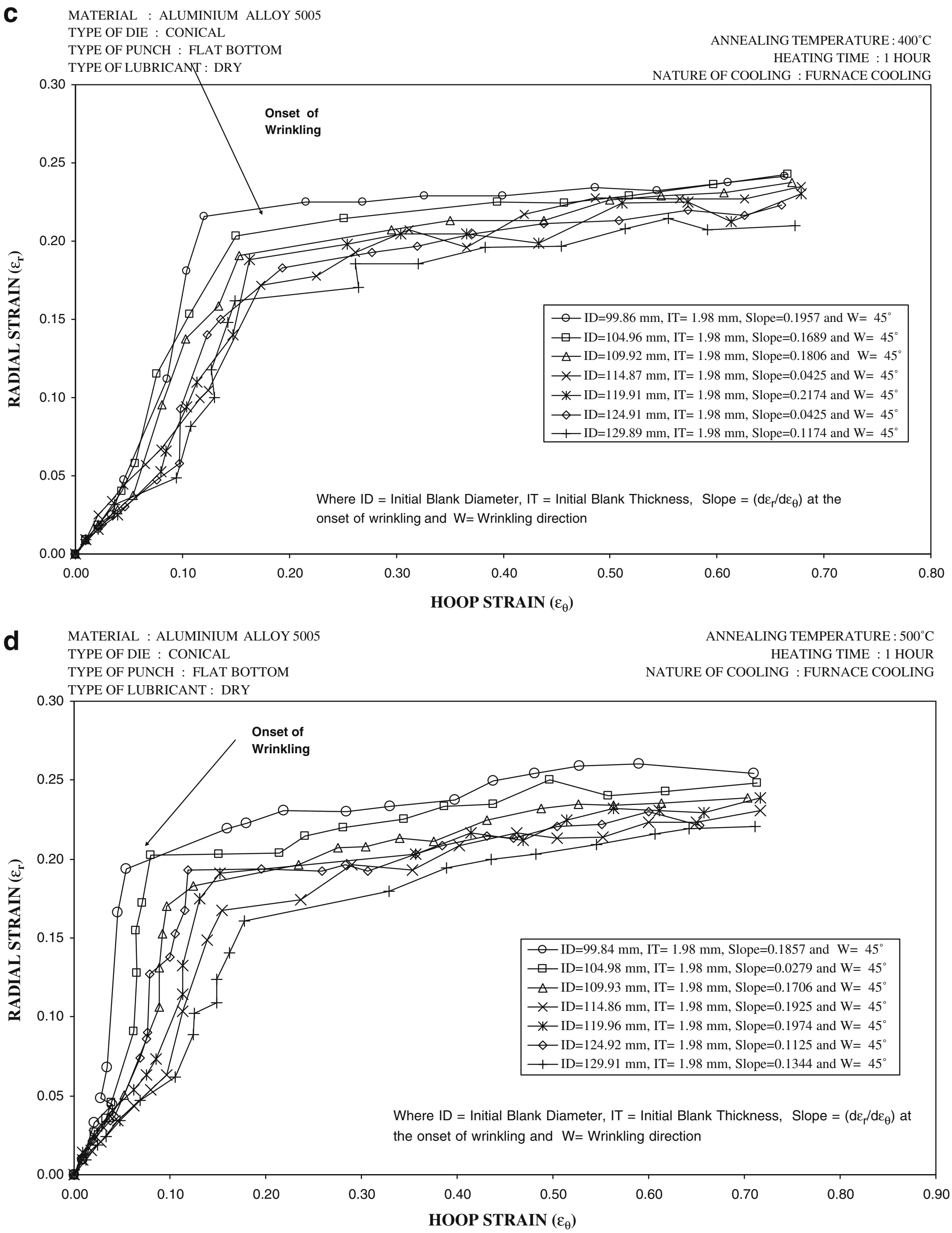

Fig. 4 (continued)

and the wrinkling region. As shown in the Fig. 9, the limiting tangent values drawn from Y and X-axis are 1.07 and 0.78 respectively and the ratio of β which is nothing but the ratio of ($d\varepsilon_\theta$ / $d\varepsilon_r$) is about 1.382. From Table 5, the theoretical value of ratio ($d\varepsilon_\theta$ / $d\varepsilon_r$) is also very close to 1.382 and therefore both the theoretical and the experimental values of β matches each other, irrespective of the different annealed temperatures.

Figure 10 has been plotted between the stress ratio, $(\tau_{\max}/\sigma_r)$ and ratio, $(\tau_{\max}/\sigma_\theta)$, obtained using Eq. (18), for

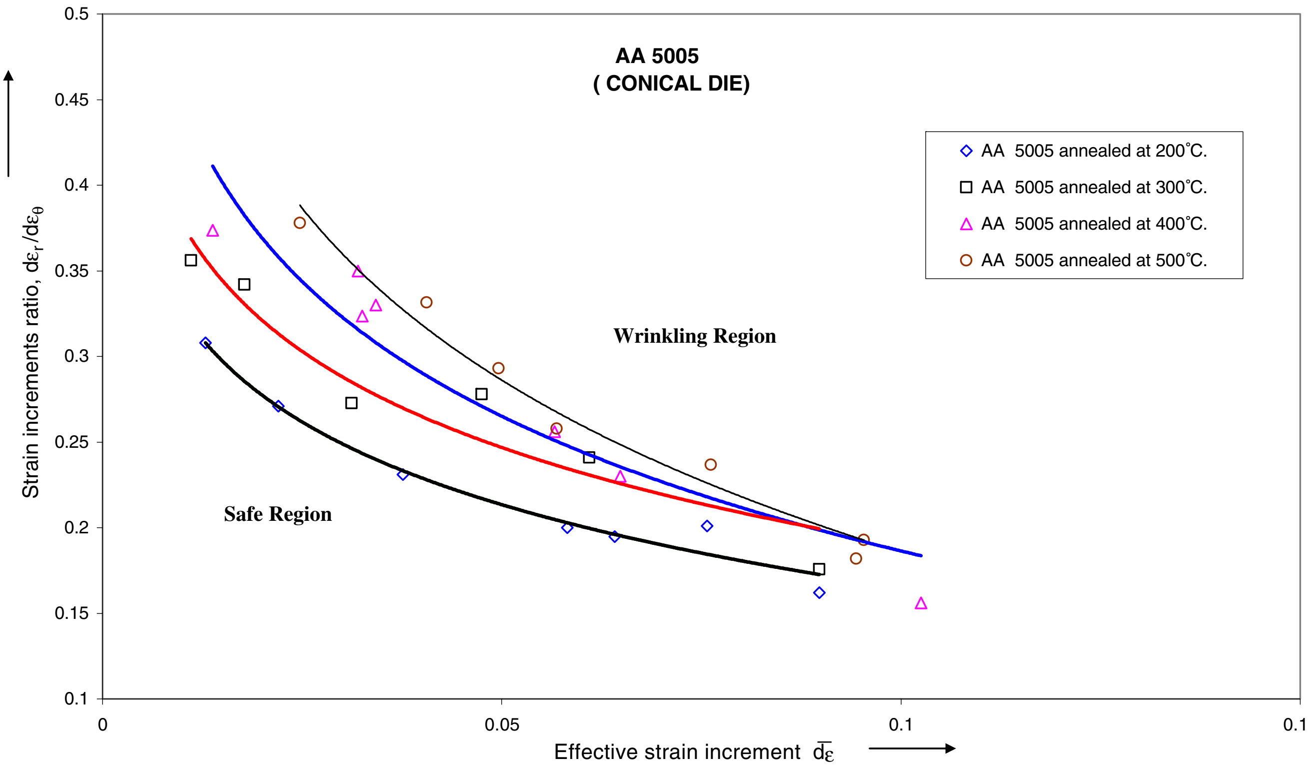

Fig. 5 Wrinkling limit diagram in terms of strain increments ratio for aluminium alloy 5005

four different annealed temperature for Aluminum alloy 5005 when drawn through Conical die. It is noted that there is a clear demarcation line or curve between the safe region and the wrinkling region. As shown in this figure, the limiting tangent values drawn from Y and X-axis are 0.93 and 0.96 respectively and the ratio of, α, which is nothing but the ratio of (σ_θ/σ_r) is about 0.967 for Conical die.

Figure 11 has been plotted between the strain ratio $(\gamma_{max}/\varepsilon_r)$ and the strain ratio $(\gamma_{max}/\varepsilon_\theta)$ obtained using Eq. (17), for four different annealed temperature for Aluminum alloy 5005 when drawn through Conical die. As mentioned earlier, there is a clear demarcation curve between the safe region and the wrinkling region for four different annealed temperature. As shown in these figures, the limiting tangent

Fig. 6 Wrinkling limit diagram in terms of stress ratio for aluminium alloy 5005

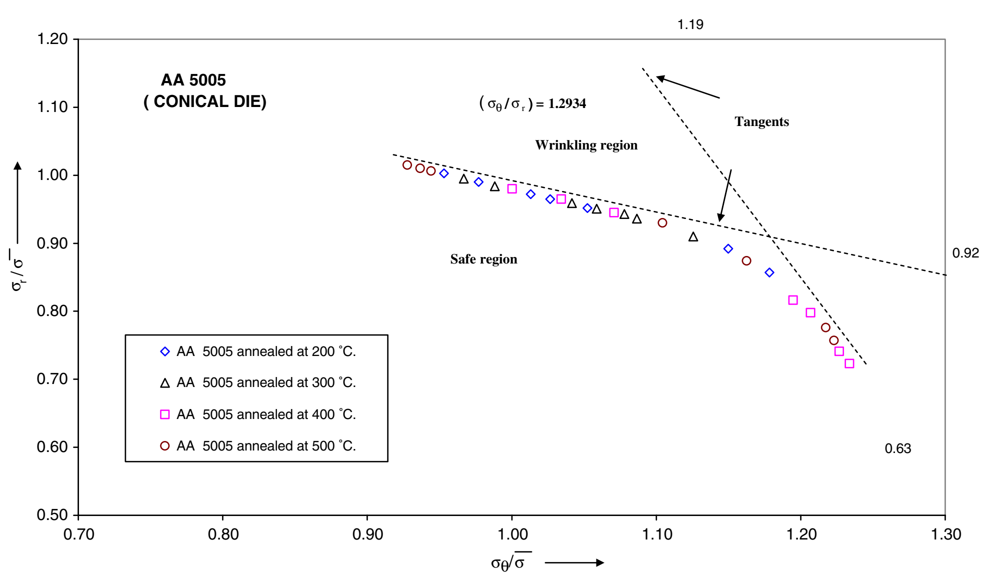

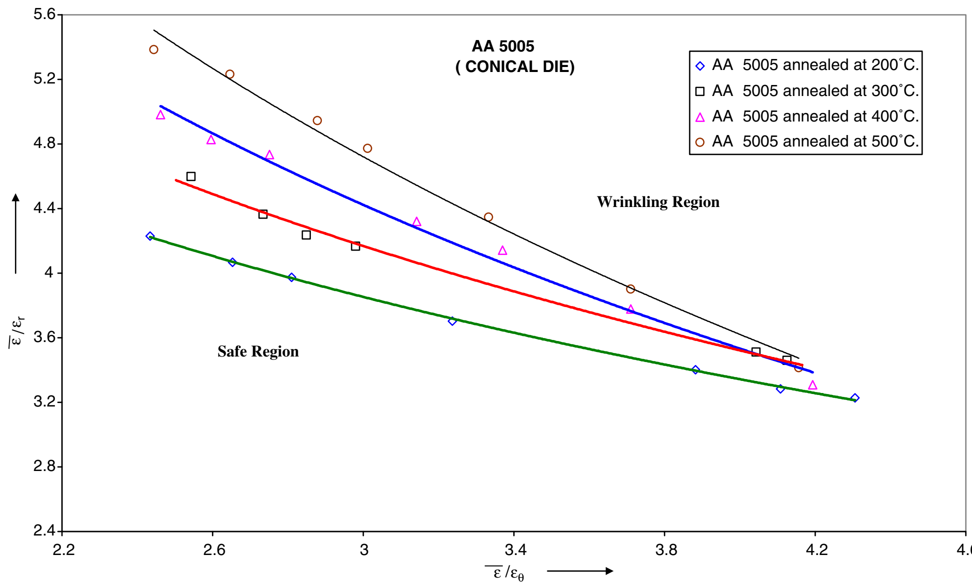

Fig. 7 Wrinkling limit diagram in terms of strain ratios for aluminium alloy 5005

values drawn from Y and X-axis are 1.20 and 0.335 respectively and the ratio of (ε_θ / ε_r) is about 3.515

Conclusions

The major conclusions that are drawn from the present experimental investigations are listed below:

- There is a definite limit curve for the onset of wrinkling which can be represented in terms of the strain increments ratio and the stress ratio.
- The Aluminum alloy 5005 annealed at temperature 500°C is superior in suppressing the wrinkles comparing with the sheets, annealed at other three temperatures.
- The wrinkling limit value (β) according to the theory and the experiment matches each other.
- Material having high n value, high R value and high UTS/ σ_y ratio suppresses the wrinkling.
- Wrinkling limit diagrams drawn in terms of strain increments ratio is highly suitable for the study of wrinkling behaviour of sheet metals

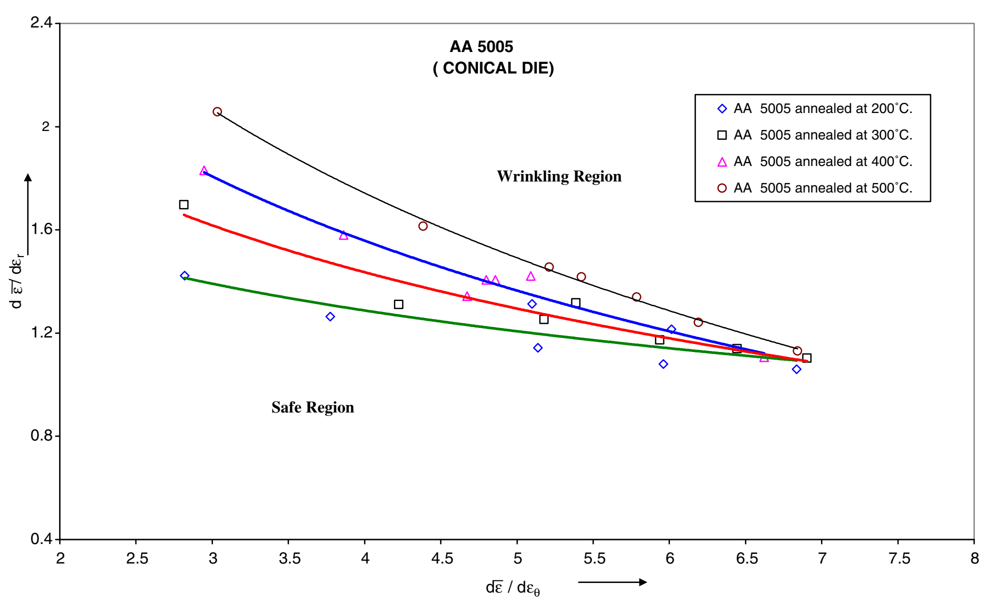

Fig. 8 Wrinkling limit diagram in terms of strain increments ratio for aluminium alloy 5005

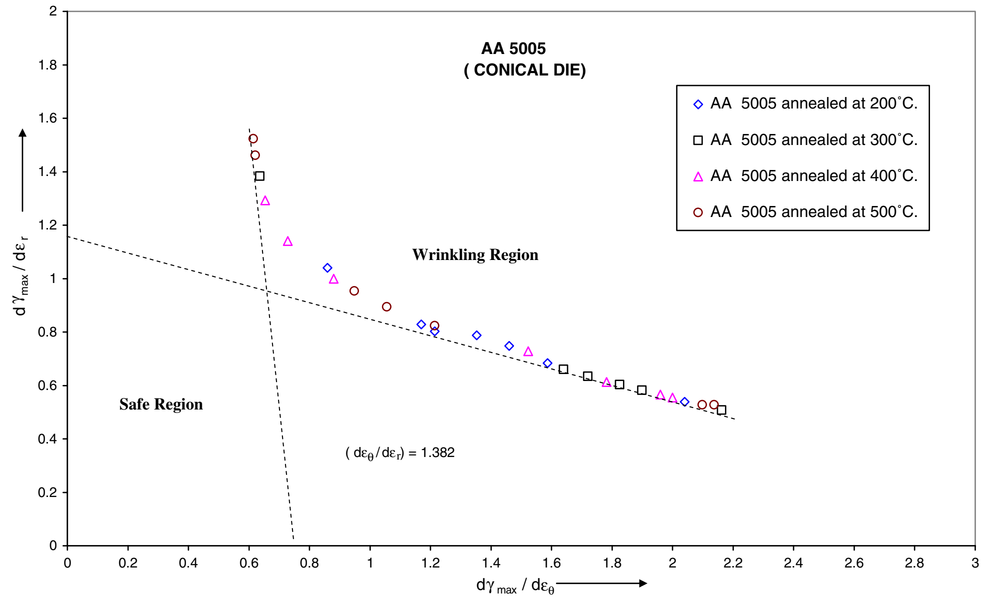

Fig. 9 Wrinkling limit diagram in terms of strain increments ratio for aluminium alloy 5005

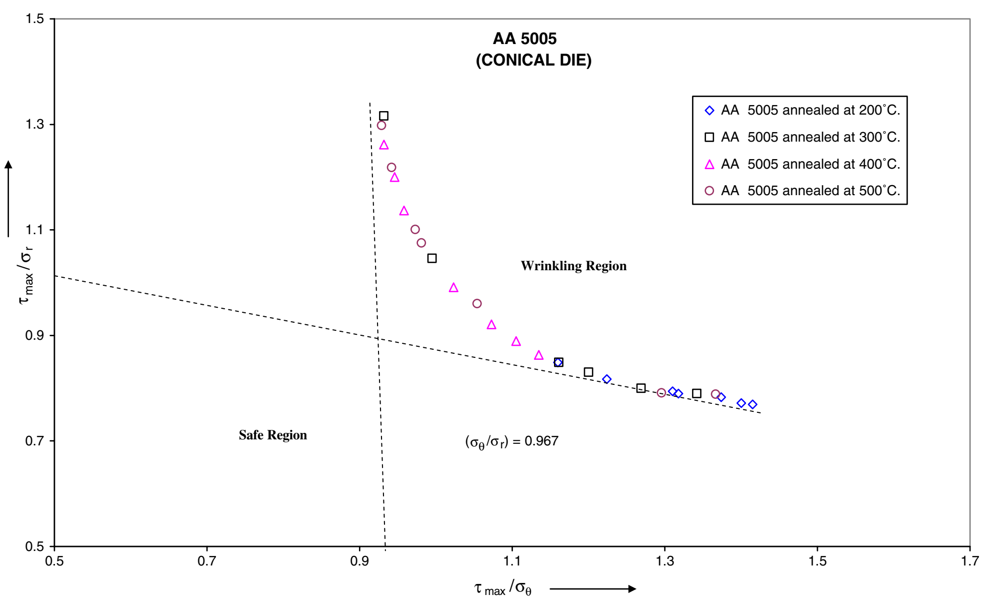

Fig. 10 Wrinkling limit diagram in terms of stress ratio for aluminium alloy 5005

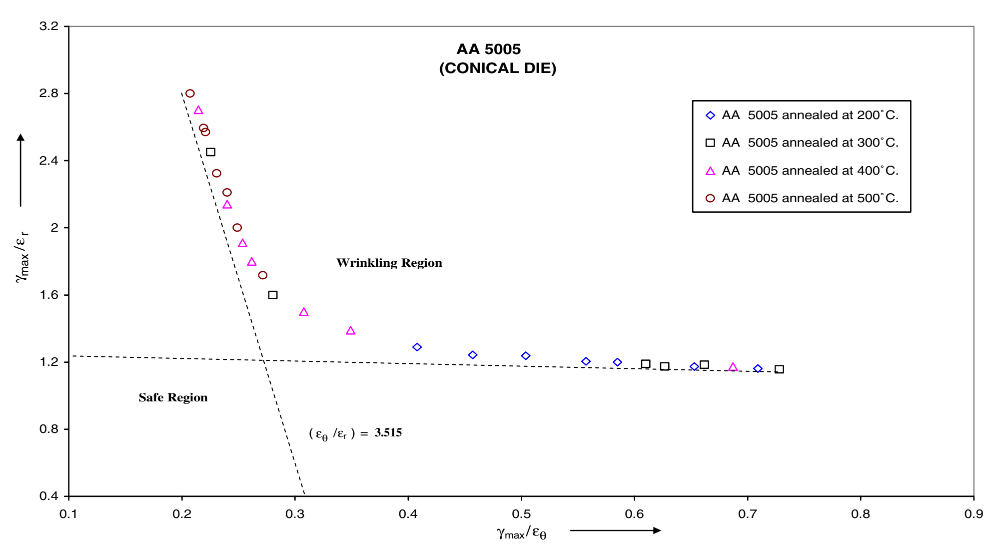

Fig. 11 Wrinkling limit diagram in terms of strain ratios for aluminium 5005 alloy

Acknowledgement The authors wish to acknowledge the help from DST and the National Facility of OIM, IIT Bombay.

References

1. Nikhil R, Raghuram T, Vamsi Krishna B, Prasad Rao K, Venugopal P (2005) Effect of cryo-rolling and annealing on microstructure and properties of commercially pure Aluminum. Mater Sci Eng A 398:246–251
2. Takuda H, Yamazaki N, Hatta N, Kikuchi S (1995) Influence of cold-rolling and annealing conditions on formability of aluminum alloy sheet. J Mater Sci 30:957–963
3. Karima M, Sowerby R (1980) Report No.144. Faculty of Engineering, McMaster University, Hamilton
4. Narayanasamy R, Sowerby R (1994) Wrinkling of sheet metals when drawing through a conical die. J Mater Proc Tech 41:275–290
5. Di S, Thomson PF (1997) Neural network approach for prediction of wrinkling limit in square metal sheet under diagonal tension. J Testing Eval, JTEVA 25(1):74–81
6. Wang J, Wu X, Thomson PF, Flitman A (2000) A Neural networks approach to investigating the geometrical influence on wrinkling in sheet metal forming. J Mater Proc Tech 105:215–220
7. Youngsuk K, Youngjin S (2000) Study on wrinkling limit diagram of anisotropic sheet metals. J Mater Proc Tech 97:88–94
8. Hill R (1950) Mathematical theory of plasticity, Ch.12. Oxford Univ. Press, London
9. Hutchinson JW (1974) Plastic buckling. In: Yin CS (ed) Advances in applied mechanics, 14, pp 215–220
10. Wang CT, Kinzel G, Altan T (1994) Wrinkling criterion for an anisotropic shell with compound curvatures I sheet forming. Int J Mater Proc Tech Sci 36(10):945–960
11. Narayanasamy R, Sathiya Narayanan C (2005) Formability of HSLA and EDDQ steels of tube products of India. Indian J Eng Mater Sci 12:141–150
12. Narayanasamy R, Loganathan C (2006) Study on wrinkling limit of commercially pure aluminum sheet metals of different grades when drawn through conical and tractrix dies. Mater Sci Eng A 419(1–2):249–261